32nd Electric Vehicle Symposium (EVS32)
Lyon, France, May 19 - 22, 2019

Design of Lightweight Electric Bus in Thailand using Composite Materials

Kitchanon Ruangjirakit[1], Pathawee Kunakorn-ong[1], Pattaramon Jongpradist[1*], Sontipee Aimmanee[1], Yossapong Laoonual[1]

[1]Department of Mechanical Engineering, Faculty of Engineering, King Mongkut's University of Technology Thonburi, Bangkok 10140, Thailand,
**corresponding author, email: pattaramon.jon@mail.kmutt.ac.th*

Summary

The Thai Government has introduced a plan to replace conventional internal combustion engine (ICE) vehicles by electric vehicles (EVs) and increase the number of PHEVs and BEVs to 1.2 million by the year 2036. Design for lightweight EVs' structures is in vital demand not only to enrich energy consumption efficiency but also to diminish the entailed battery capacity for a long driving range. To align with this development, this paper aims to propose a novel preliminary design methodology for electric bus structures by implementing the finite-element method via ABAQUS™. The monocoque sandwich-structured fiber-reinforced composite bus is designed to cover a minimum driving range of 300 km. The bus body is designed based on many criteria, such as Thai vehicle registration regulations, the strength of the bus structure under various driving conditions, bending and torsion stiffness requirements and the requirement of rollover test according to UN ECE R66. Presented is the procedure of a variation of sandwich core and face thicknesses in form of multivariate functions to predict the structural responses. The critical areas in design under bending condition are the floor panel and its edges under the battery packs, whereas in rollover analysis the critical areas are at the pillar joints, which are under shear loads. The proposed preliminary design passes all requirements and delivers a reduction in the body mass by 36% compared to the benchmark one.

Keywords: EV (Electric vehicle), bus, finite element calculation, safety, public transport

1 Introduction

Global warming crisis has become a serious issue of the world community. The International Energy Agency (IEA) [1] proposed the two-degree Celsius Scenario (2DS) that limits the average global temperature increase to only 2°C in 2050. Transport sector is a significant contributor towards the success of 2DS in which CO_2 emission is aimed to be reduced by 21%. In Thailand, the government has proposed a plan to gradually replace diesel buses with electric buses and relevant policies have been introduced in order to promote the production capacity of Thai manufacturers to 1,000 electric buses annually.

At the upstream level of production, proper engineering analysis plays a very important role in electric bus design. Electric bus structures differ from those of conventional buses due to the presence of heavy components such as batteries and the absence of the internal combustion engines as well as their associated accessories. This brings to the significance of light and compact structural design. Lightweight structures are also important for long-range electric vehicles, since they increase energy consumption efficiency and decrease the required battery capacity. Consequently, many modern automotive industries have reduced weights of vehicles by replacing some parts previously made by metal with fiber-reinforced composites, due to the latter having higher strength and stiffness to weight ratios. Besides those superior characteristics, fiber-reinforced composites offer advantages in design flexibility, complex shape manufacturability, and properties tailorability, which all are necessary for automotive structure development.

For decades, studies of vehicle structure integrity have been conducted by many researchers [2-6]. However, most of them focused on conventional metal spaceframes. Less attentions were paid to composite monocoque structures, which integrate the chassis with the body, especially for heavy-duty vehicles due to their comparatively sophisticated design methodology. Instead, only individual composite part or small monocoque were commonly investigated. For instance, Ko, et al. [7] studied the crashworthiness of sandwich composite bus with crash conditions; frontal crash and roll-over test. According to the structural details, the structure is not classified as a chassis-less structure because there exist metal extruded profiles used as a skeleton. Velea, et al. [8] designed a unibody compact vehicle by implementing multi-objective genetic optimization to define a material distribution of fiber reinforced polymers. The trade-off plots compromise between multi-objective satisfactions. Testoni, [9] proposed sandwich structure usage for an urban electric bus. The design focused on development of the monocoque concept. The bus structure was subjected to the normal working loads and quasi-static force acted on the roof's corner representing roll-over crash in compliance with UN ECE R66. The additional plies of unidirectional carbon fiber were used to reduce an excessive strain values for the pillar and window regions. Based on these literatures, the design of composite monocoque structures for large vehicles, such as buses is not adequately studied and published. In addition, applications of advanced optimization tools could frequently provide impractical or cumbersome implementations to manufacturers and technicians. Thus, a fundamental yet systematic methodology to reduce weight of automotive body is also necessary for preliminary design purpose.

In order to fill the above research gaps, this paper proposes a design of an 8-m electric bus structure with 300-km range using composite materials. Strength and crashworthiness of the electric bus structure are analyzed by finite element method via ABAQUS/Standard and ABAQUS/Explicit solvers. The design criteria include bus specifications based on Thai vehicle registration regulations, the strength of the bus under road driving conditions, the bending and torsion stiffness and rollover test according to UN ECE Regulation No. 66 [10]. A novel design methodology presented in form of performance sensitivity equations is finally proposed to readily search for the expected bus structural responses under the most effective options of mass reduction.

2 Numerical Model

2.1 General description of electric bus

The electric bus considered herein is designed for intercity transport and multi-purpose utilization with capacity of 24 seated passengers. The dimensions of the bus are 2.55 meters wide, 8 meters long, and 3.2 meters high. Figure 1 illustrates an outside perspective and components of the bus model. As seen, the bus consists of a monocoque structure separated into the top part shown in grey and the bottom part shown in orange. The top part also includes the cover panel of an air conditioner, while the bottom part is connected to the front and rear axles. The openings are purposely for passenger's door, emergency exit, and windows. The bus interior comprises of passenger seats that are anchored to the floor panel. The battery packs are stored in the compartment beneath the floor. The bus is planned to run on a maximum distance of 300 kilometers per charge. To specify the required battery capacity for the present electric bus, the relations between energy consumption and gross vehicle weight (GVW) of other electric buses currently in service [11-16] are plotted in Fig. 2. The GVW of an 8-m bus is estimated to be 8.8 tons as indicated in Table 1. The energy consumption based on scaling analysis is thus projected to be approximately

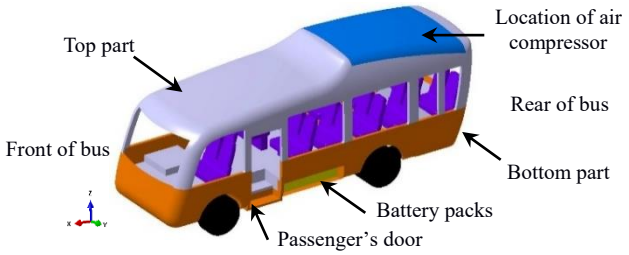

Figure 1: Components on electric bus

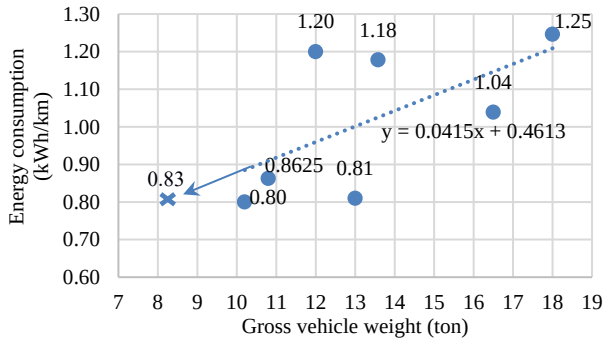

Figure 2: Relation between gross vehicle weight of electric buses and energy consumption

Table1: Mass distribution of bus components

Item	Weight (kg)
Rear axle (in-wheel motors)	950
Front axle	482
12 double seats and driver seat	407
Tire 265/70 R19.5	540
Passengers	1,875
Air conditioning system	180
Battery (320 kWh)	1,280
Bus structure	2,806
2 Passenger doors	230
Windows	230
Total	8,774

0.83 kWh/km and the required battery capacity is 249 kWh. Since the battery should remain at least 20% at a specified maximum driving range, the actual battery capacity becomes 320 kWh. With an energy density of 250 Wh/kg, the total mass of battery is estimated as 1,280 kg. The breakdown mass distribution of the electric bus components is then initially listed in Table 1. As seen, the 2,806-kg mass structure is used as a benchmark in this paper.

2.2 Material properties

Almost all parts of the bus monocoque are made of sandwich structures, in which foam core is DIAB DIVINYCELL H100 [17] and faces are woven E-glass/epoxy. Only the roof cover of the top part is composed of woven E-glass fiber-reinforced epoxy laminate. Three types of plain weave roving, i.e. glass cloth with density of 400 g/m^2 (G400), glass cloth 600 g/m^2 (G600) and carbon cloth 200 g/m^2 (C200) are

Table2: Mechanical properties of laminated composite materials

Material properties	G400	G600	C200
Tensile modulus, E_1 (MPa)	18,036	16,281	78,493
Transverse modulus, E_2 (MPa)	18,036	16,281	78,493
In-plane shear modulus, G_{12} (MPa)	2,219	2,942	2,122
Poisson's ratio (In-plane), ν_{12}	0.053	0.04	0.052
Longitudinal tensile strength, F_{1t} (MPa)	206.6	309	411.4
Longitudinal compressive strength, F_{1c} (MPa)	97.8	195	370.6
Transverse tensile strength, F_{2t} (MPa)	206.6	309	411.4
Transverse compressive strength, F_{2c} (MPa)	97.8	195	370.6
In-Plane shear strength, S_{12} (MPa)	27.45	27.9	22.38
Density (kg/m^3)	1,588	1,717	1,336

Table3: Mechanical properties of H100 Foam [17]

Compressive strength (MPa)	1.65
Compressive modulus (MPa)	115
Tensile strength (MPa)	2.5
Tensile modulus (MPa)	105
Shear strength (MPa)	35
Shear modulus (MPa)	28
Density (kg/m^3)	100

selected for the bus design. Mechanical properties of these laminated composites were obtained from testing according to the ASTM standards; ASTM D3039 for tensile properties, ASTM D3410 for compressive properties and ASTM D3518 for in-plane shear properties. The material properties of laminated composite materials and foam are tabulated in Tables 2 and 3, respectively.

2.3 Design criteria

While a bus is traveling on the road, the loading conditions are similar to other types of vehicles. The major differences in loads exerted on electric vehicles are the powertrain components, layout of subsystems, battery compartment, and the regulatory frameworks on required equipment and safety. In the current work, the design criteria are established based upon three distinct aspects; 1) to represent the real driving conditions, 2) to follow the recommended structural strength and stiffness under normal operating conditions, and 3) to include the safety concern under the rollover accident. As a result, the loadings and constraints in finite-element analysis are listed as follows;

1. Longitudinal loading is applied to represent the conditions when the bus is accelerated or decelerated during rectilinear motions. The equivalent gravitational load of 0.75g along the longitudinal direction is exerted on the entire bus structure while all wheels of the bus are simply modelled as pinned supports at wheel shafts. Safety factor (SF) of 2 is used in the design considering the maximum stress in the structure.

2. Lateral loading occurs during turning of the bus. The body force due to acceleration of 0.75g in transverse direction is imposed on the bus structure whereas the boundary conditions and constraints are similar to the case of longitudinal loading. The SF of 2 is also employed.

3. Natural frequency of the bus structure is taken into consideration for the resonance that may occur due to road-induced vibration. In design of the bus body, the first natural frequency in structural mode should be higher than 5 Hz [4].

4. Bending stiffness (K_B) is the ability of structure to carry heavy passenger loads and other components such as battery packs, air conditioning system and its own weight. Displayed in Fig. 3(a), all the wheels are constrained as pin supports. The value of K_B is calculated by using the maximum deflection of structure under the bending case as expressed in Equation (1).

$$K_B = W(\frac{1}{d_{\max}}) \tag{1}$$

In the above equation, W is the gross vehicle weight of the bus structure, d_{max} the maximum deformation on the structure under bending load. The criterion of required bending stiffness is 36,000 N/mm. This value is determined based on dimensions of bus and resonance frequency given in [18].

5. Torsional stiffness (K_T) contributes to the ability of the bus structure to resist twisting load due to uneven road surface. To evaluate K_T, a vertical displacement is applied to the front left wheel of structure while the other three wheels are pinned as shown in Fig.3(b). The wheel constraint condition results in a twisting angle θ measured at the front axle. The K_T is

$$K_T = \frac{Ft}{\theta} \tag{2}$$

where t is the length of the front axle and F is reaction force at front left wheel. The recommendation of torsional stiffness is 40,000 Nm/deg [19].

6. Rollover test based on UN ECE Regulation No. 66 [10] concerns the impact resistance and strength of superstructure of large passenger vehicles carrying more than 22 passengers excluding driver and crew under rollover accident. In the test procedure, the bus is positioned on a rigid tilting platform rotating at 5 degree per second until the bus is unstable and rollover onto the ground that is 800-mm below the platform as depicted in Fig. 4. In order to comply with the regulation, safety space or residual space is defined as the safe area provided for occupants during the roll-over test. The safety space must be preserved and must not be invaded by any structural members throughout the test event.

The initiation of material failure is detected by Hashin criteria [20] implementing a two-dimensional classical lamination approach with ply discounting as the material degrades. Four different damage initiation mechanisms are included:

Tensile mode in principal material coordinate $(\sigma_{11} \geq 0)$:

$$F_f^t = (\frac{\sigma_{11}}{F_{1t}})^2 \quad (3)$$

Compressive mode in principal material coordinate $(\sigma_{11} < 0)$:

$$F_f^c = (\frac{\sigma_{11}}{F_{1c}})^2 \quad (4)$$

Tensile mode perpendicular to principal material coordinate $(\sigma_{22} \geq 0)$:

$$F_m^t = (\frac{\sigma_{22}}{F_{2t}})^2 + (\frac{\sigma_{12}}{S_{12}})^2 \quad (5)$$

Compressive mode perpendicular to principal material coordinate $(\sigma_{22} < 0)$:

$$F_m^c = (\frac{\sigma_{22}}{2S_{12}})^2 + \left[\left(\frac{F_{2c}}{2S_{12}}\right)^2 - 1\right]\frac{\sigma_{22}}{F_{2c}} + (\frac{\sigma_{12}}{S_{12}})^2 \quad (6)$$

where σ_{11}, σ_{22}, and σ_{12} are the in-plane longitudinal, transverse, and shear stresses, respectively. The definition of strength variables is declared in Table 2.

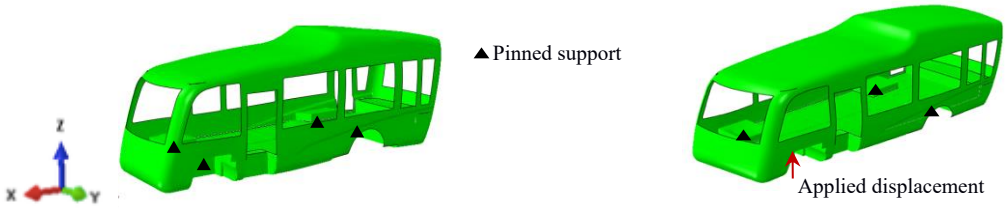

(a) (b)

Figure 3: Boundary conditions for (a) bending case (b) torsional case

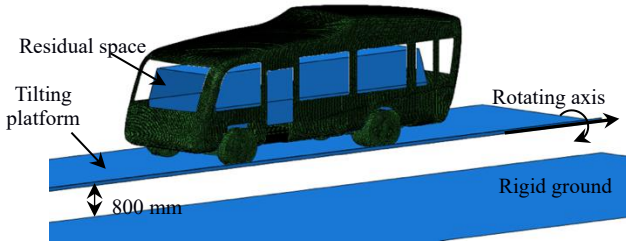

Figure 4: Rollover test components

2.4 Structural analysis of FE bus model

This section describes an overall structural integrity of the microbus in Figure 1 under design criteria described in the previous section. Stress distributions, damages, and deflections of the bus structure are mainly investigated. The bus body are partitioned into regions based on specific part's behaviors under various loads and load paths. Initially, 6-mm G400/epoxy face and 20-mm foam core are assigned to the entire bus components as the first model in the analysis stage. The FE model of bus is meshed with 3-node and 4-node shell elements with element size of 20-30 mm. The principal material coordinate of fiber of bus pillars is oriented along the vertical direction (*Z* axis in Figure 3) and that of the roof region is aligned in the transverse direction (*Y* axis) whereas, for the rest of bus, the principal fiber coordinate is assigned in the *X* axis. The material properties have been assigned through the composite layup feature in finite element Abaqus/Standard and Abaqus/Explicit solvers.

The analysis results according to six design criteria are illustrated in Figure 5. Figure 5(a) shows stress distribution in the *X* axis under longitudinal load. Stress concentrations are noticed at the discontinuous areas on the side structure and along the upper and lower rims of window frames. For lateral case in Fig. 5(b), higher stresses are observed at pillars especially in the direction of the bus height (Z axis). The SF of each loading is more than the allowable criteria of 2. Under the bending and torsion load cases, the vertical

deflections of bus structure are of primary interest because the stresses are marginal. Fig. 5(c) shows that under bending load, the largest deformation localizes at the positions of battery packs where the maximum deflection is 5.4 mm, resulting in K_B from Equation (1) of 18,600 N/mm – almost two times as low as the bending stiffness criteria. The deformation contour of torsional case is presented in Fig. 6(d). The reaction force at the wheel F is measured to be 19.6 kN and the corresponding K_T is 97,500 N.m/deg – much higher than the torsion stiffness criteria. The first modes of bending and torsion are determined from modal analysis as 13 and 19.3 Hz, respectively. They are above the criteria in section 2.3.3.

Rollover simulation is started from the unstable tilt angle (55 degree from horizontal) at time instant of 0 second (Fig. 6) and the bus falls onto the ground under gravity. The bus impacts the ground at time instant of 2.55 seconds and thereafter slides on the ground for a short interval. The deformation of bus structure reaches its maximum at the time instant of 2.66 seconds. The simulation is terminated at t = 3.08 seconds when the bus rests on the floor. Rollover results at the instant of maximum deformation is displayed in Fig. 7. As seen, the joints between pillars and side panels on both sides are prone to damage in the longitudinal direction as shown in red contour in Figure 7. However, for the woven composite laminate, there exist fibers aligned in that direction and therefore the particular locations still have the ability to withstand the loads. The deformations are measured in terms of a clearance distance between the deformed bus structure and the residual space. The minimum clearance at the second to last pillar is found to be 65 mm inferring that the first bus model passes the UN ECE regulation.

Although structures did not intrude into the safety space during rollover test, the distribution of stress should be studied. Fig. 9 shows some examples of stress contour when the maximum deformation occurs. It is noticed that longitudinal stress (σ_{11}) is concentrated on an outer laminated layer of the structure at the front and rear pillars as shown in Fig. 9 (a) while stress (σ_{22}) is perpendicularly present on an inner laminated layer on the pillar adjacent to passenger door.

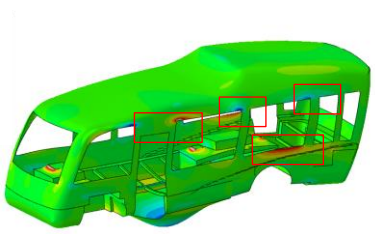

(a) Stress distribution (σ_{11}) under longitudinal load

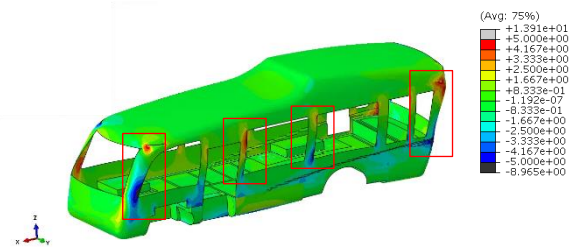

(b) Stress distribution (σ_{22}) under lateral load

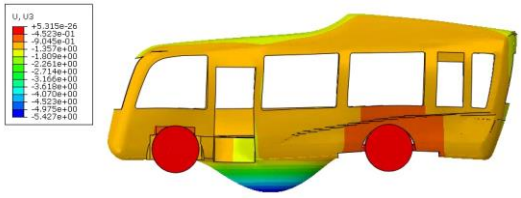

(c) Deflection under bending

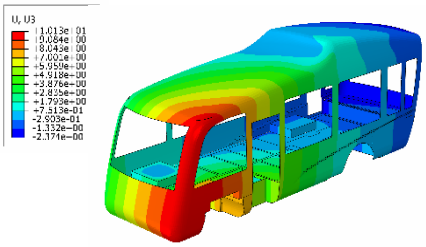

(d) Deflection under torsion

Figure 5: Analysis results

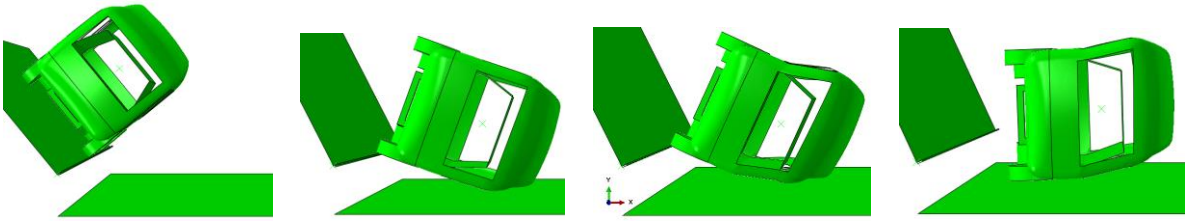

t = 0 sec t = 2.55 sec t = 2.66 sec t = 3.08 sec

Figure 6: Rollover results

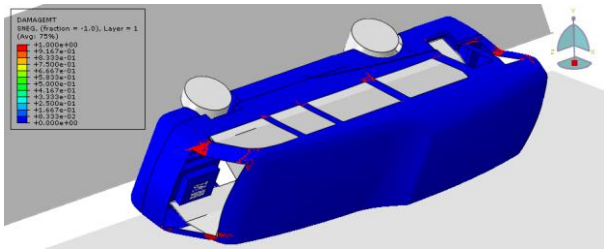

Figure 7: Tension damage in transverse direction to the axial of the pillars at the instance of maximum deformation

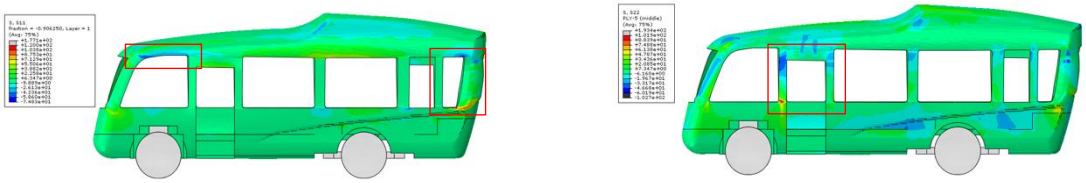

(a) σ_{11} on outer structure (b) σ_{22} on inner structure

Figure 8: Stress distribution on side structure at maximum deformation

According to considerations of stress localizations under each load case, stress intensities are obviously observed on the side structures. In addition, in view of the manufacturing process, the bus monocoque is designed to be assembled by using top and bottom molds. The bus structure is therefore partitioned into 7 components as shown in Fig. 9. Pillar structures shown as yellow areas in Fig. 9(a) are the main component to resist the impact from rollover test. Side panels shown in pink are the side structure in which less stress intensities are noticed in the former analysis. Bottom structure (grey area) is the base structure supporting the driving system. Since large deformations are noticed at the area that support heavy battery packs, the battery tray area (area bounded by dash lines) is separated as another component from the bottom part. Floor structure is a composite sandwich placed on top of the bottom structure to carry the passenger compartment loads. Roof cover shown Fig. 10(b) is designed as a laminated composite without a core and ceiling (Fig. 10c) is the structure for air conditioner's installation underneath the roof cover.

From the analysis results, since the bending stiffness of the bus is extremely insufficient due to a large deformation at the battery tray location. The area is first redesigned by partially replacing the face material of G400 by C200 that provides higher modulus and also increase the core thickness. The face's material of the pillars is also changed to G600 which offers superior maximum strength in both tensile and compressive modes. The recent material assignments on the bus structure are presented in Fig. 10. After the FE analysis, the deformation of battery tray is reduced to 2.6 mm and K_B is calculated as 32,042 N/mm. This modified model is later on called the 'baseline model' and will be used for parametric study in the next section.

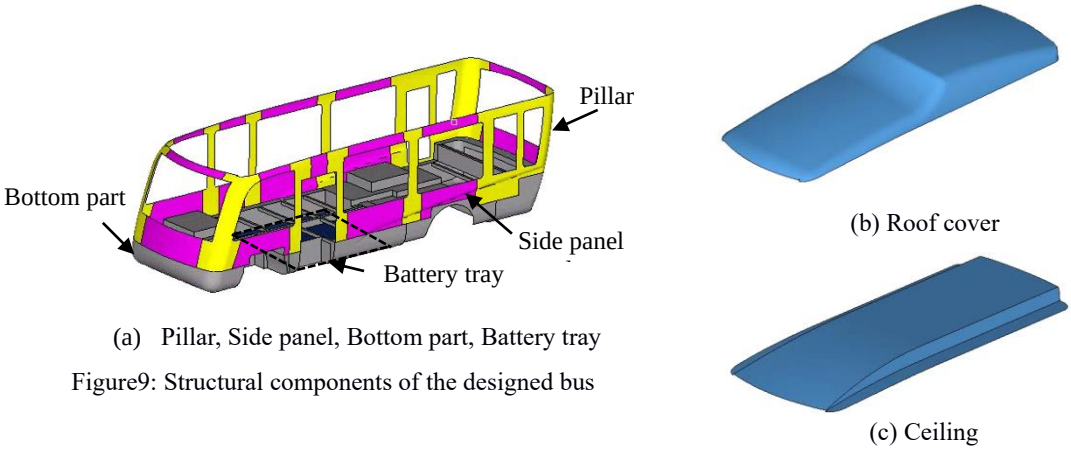

(a) Pillar, Side panel, Bottom part, Battery tray

(b) Roof cover

(c) Ceiling

Figure9: Structural components of the designed bus

<table>
<tr><td colspan="3">Bottom part | Side panel | Floor</td><td>Pillar</td><td>Battery tray</td><td>Ceiling</td><td>Roof cover</td></tr>
<tr><td colspan="3" rowspan="2">G400, t = 6 mm</td><td rowspan="2">G600, t = 6 mm</td><td>C200, t = 4 mm</td><td rowspan="2">G400, t = 6 mm</td><td rowspan="2">G400, t = 6 mm</td></tr>
<tr><td>G400, t = 2 mm</td></tr>
<tr><td colspan="3">Foam, t = 20 mm</td><td>Foam, t = 20 mm</td><td>Foam, t = 30 mm</td><td>Foam, t = 50 mm</td><td rowspan="2"></td></tr>
<tr><td colspan="3" rowspan="2">G400, t = 6 mm</td><td rowspan="2">G600, t = 6 mm</td><td>G400, t = 2 mm</td><td rowspan="2">G400, t = 6 mm</td></tr>
<tr><td>C200, t = 4 mm</td></tr>
</table>

Figure10: Materials assignment for baseline model

3 Parametric Study on Structural Stiffness

In the design process, it is essential to identify the level of significance of the design variables so as to achieve an optimal design based on the design objectives. One of the challenges in designing a composite sandwich structure is the multi-parameters contributing to the response of interest. In particular, strength and stiffness as well as minimal material weight and cost can be tailored through the material selection, material properties, thickness and stacking sequence. In the design of lightweight monocoque bus structure, evaluation of significant parameters and a parametric study on the effects of each design variable to the structural performance of the bus body is thus vital.

3.1 Methodology for structural parametric study

In this research, a parametric study is conducted by changing the thickness of sandwich's core and face of the designed components. The responses of interest are the bending and torsional stiffnesses of the bus monocoque structure compared to that of the baseline model. The effects of the variation in thickness are examined by either increasing the core thickness of each component by 10 mm or reducing the face's thickness on each side of the sandwich structure by 3 mm while other variables remain unchanged. For the battery tray in which the materials are different from other components, the thickness of G400 and C200 layers are reduced by a half.

The analysis results from parametric study are plotted in terms of the changes in bending stiffness (ΔK_B) and torsional stiffness (ΔK_T) versus the variation in the component's mass (ΔM) compared with those of the baseline model as shown in Fig. 11 and Fig. 12. The letters "C" and "F" in the figures indicate the results obtained from changing the core thickness (Δt_C) and the face thickness (Δt_F), respectively. The reference point of the baseline model lays on the origin of the coordinate system. Alteration of the face thickness results in a considerably larger change in the component mass as compared to the change in the core thickness. The sensitivity analysis results show that an increase in the core thickness increases both the mass and the structural stiffness as can be seen from the data points that lie in the first quadrant of the graph. When comparing each of the Δt_C data point to the origin, the points exhibiting a higher slope contribute to a more favorable change in stiffness to mass ratio. The effects of decreasing the face thickness, on the other hand, results in the points lying in the third quadrant, which means that although a reduction in component's mass can be achieved, the structural stiffness is also compromised. For the Δt_F case, more prominent effects are found in the change of mass. Hence, the Δt_F data points that lie farther from the vertical axis and close to the horizontal axis are preferred as the decrease in structural mass is realized while the deteriorating effect of decreasing bending and torsional stiffness is minimized.

The normalization of the change in stiffnesses with respect to the component mass ($\Delta K/\Delta M$), hereafter referred to as specific stiffness, are summarized in Table 4. The numbers in bold font in the table indicate the greatest effect of the design parameters (changes in core and face thicknesses) on the specific stiffness and mass change. It is obviously observed that, for a unit change of structural mass, Δt_C generally offers higher specific stiffness than Δt_F whereas Δt_F commonly affects higher mass change. The most significant parameters to the bending specific stiffness, torsion specific stiffness and mass are $\Delta t_{C,\ Battery\ tray}$, $\Delta t_{C,\ Bottom\ part}$, and $\Delta t_{F,\ Bottom\ part}$, respectively. In summary, if the improvement in stiffness is required while the body mass is also of concern, increase in the core thickness is recommended, particularly for the battery tray. Since only slight effects to both stiffnesses are found for Δt_F, changes in face thickness of some components such as the bottom part and ceiling that principally lessen the structural mass are suitable adoptions for lightweight design.

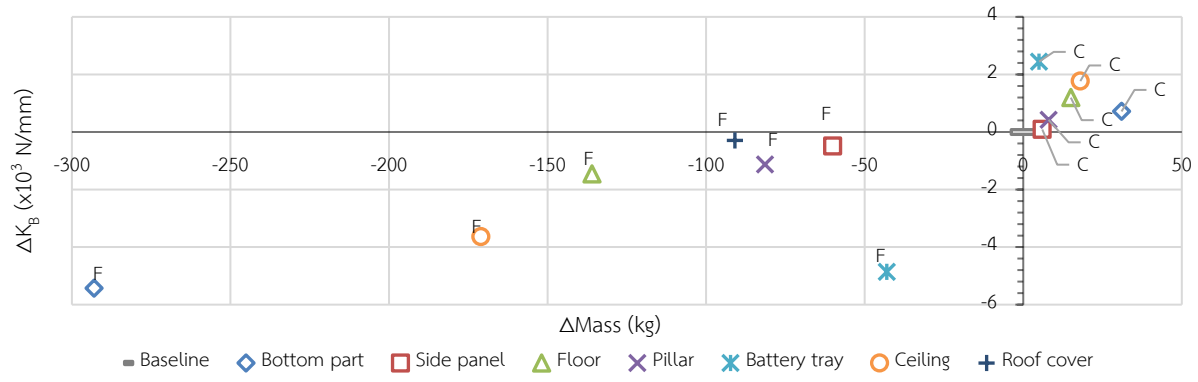

Figure11: Parametric study for K_B

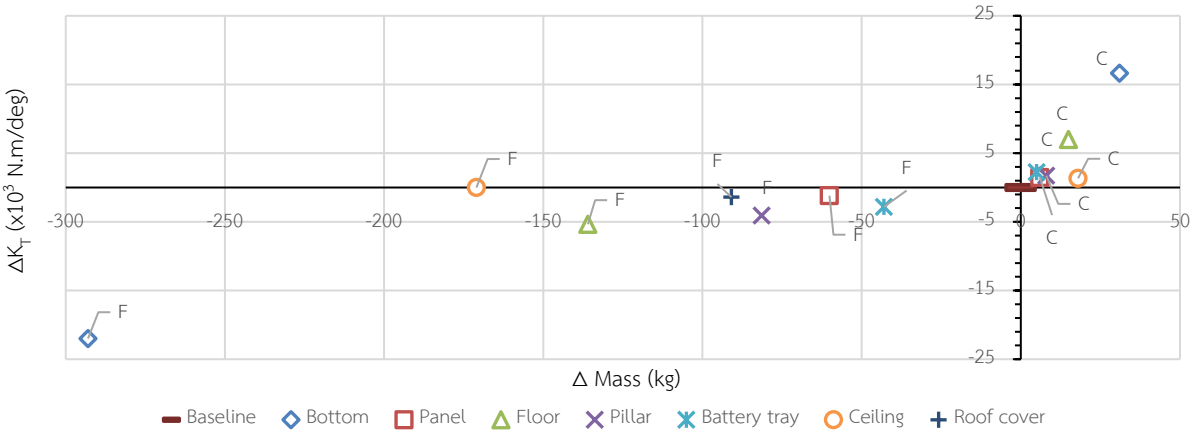

Figure12: Parametric study for K_T

Table4: Specific bending and torsional stiffnesses

Component	Δt_C = 10 mm					Δt_F = -3 mm/face				
	ΔM	ΔK_B	ΔK_T	$\Delta K_B/\Delta M$	$\Delta K_T/\Delta M$	ΔM	ΔK_B	ΔK_T	$\Delta K_B/\Delta M$	$\Delta K_T/\Delta M$
Bottom part	31	714	16645	23.0	**536.9**	**-293**	-5429	-21988	18.5	75.0
Side panel	6	88	1458	14.7	242.9	-60	-490	-1194	8.2	19.9
Floor	15	1194	6997	79.6	466.5	-136	-1457	-5350	10.7	39.3
Pillar	8	423	1718	52.8	214.7	-81	-1128	-4081	13.9	50.1
Battery tray	5	2443	2231	**488.7**	446.1	-43	-4863	-2826	113.1	65.7
Ceiling	18	1768	1341	98.2	74.5	-171	-3639	0	21.3	0
Roof cover	No core for this component					-91	-294	-1403	3.2	15.4

Note: units of ΔM is kg, ΔK_B is N/mm, ΔK_T is N.m/deg, $\Delta K_B/\Delta M$ is N/mm/kg and $\Delta K_T/\Delta M$ is N.m/deg/kg

From the parametric studies, functions of structural mass and stiffness can be linearly formulated in terms of Δt_C and Δt_F of each design component as follows:

$$\begin{bmatrix} Mass \\ K_B \\ K_T \end{bmatrix} = \begin{bmatrix} 1841 \\ 32042 \\ 95787 \end{bmatrix} + \begin{bmatrix} 3.1 & 0.6 & 1.5 & 0.8 & 0.5 & 1.8 \\ 71.4 & 8.8 & 119.4 & 42.3 & 244.3 & 176.8 \\ 1664.5 & 145.8 & 699.7 & 171.8 & 223.1 & 134.1 \end{bmatrix} \begin{bmatrix} \Delta t_{C,Bottom} \\ \Delta t_{C,Panel} \\ \Delta t_{C,Floor} \\ \Delta t_{C,Pillar} \\ \Delta t_{C,BatteryTray} \\ \Delta t_{C,Ceiling} \end{bmatrix} \quad (7)$$

$$+ \begin{bmatrix} 48.8 & 10 & 22.7 & 13.6 & 7.2 & 28.5 & 30.3 \\ 904.9 & 81.7 & 242.8 & 187.9 & 810.5 & 606.6 & 98.1 \\ 3664.7 & 199.1 & 891.6 & 680.6 & 471.1 & 0 & 467.7 \end{bmatrix} \begin{bmatrix} \Delta t_{F,Bottom} \\ \Delta t_{F,Panel} \\ \Delta t_{F,Floor} \\ \Delta t_{F,Pillar} \\ \Delta t_{F,BatteryTray} \\ \Delta t_{F,Ceiling} \\ \Delta t_{F,RoofCover} \end{bmatrix}$$

The established functions can be used to estimate the mass and stiffness of the bus structure for different design parameters without performing FE analyses. Constant terms are the values from the baseline model and the coefficients are obtained from thickness normalization. When a particular set of design variables is specified, the equations can be applied to preliminarily predict structural responses based on the selections and requirements.

3.2 Design improvement and discussion

The bending and torsion stiffnesses of the baseline bus structure are 32,042 N/mm and 95,787 N.mm/deg, respectively. The requirements entail an increase in K_B by approximately 4,000 N/mm while K_T exceeds the requirement by 45,787 N.m/deg. Table 4 and the generated response functions (Eq. 7) from the previous parametric studies are implemented to improve the design of lightweight bus structure. To enhance the K_B of the bus body, the parameters with high specific K_B are considered. The core thicknesses of floor structure, pillar, and battery tray are therefore increased by 20, 10, and 10 mm. It should be remarked that although ceiling structure offers high specific K_B, the total thickness of ceiling part is currently 62 mm which is sufficient to support air conditioner's weight.

Lightweight design of the bus body can be primarily achieved by reducing the face thicknesses of sandwich structures. In which case, considerations focus on the changes in structural mass without compromising the bending stiffness. It is noticed that benefits from the reduction in face thickness the most are the roof structure and side panel as the bending stiffness is insensitive to the change in face thickness and a similar outcome can also be observed in the torsion case. Therefore, the face thicknesses of roof cover and side panel structure are both decreased by 2 mm on each side. The proposed materials for bus structure are shown in Fig. 14. The anticipated K_B and K_T obtained from Eq. 7 are 36,772 N/mm and 111,998 N.m/deg which pass the stiffness requirements. The structural mass of the new design is 1,783 kg which is 3.2% less than the baseline bus model. As the mass of structure evaluated from the existing models in Table. 1, the mass of bus structure is 36% less than benchmark one.

The suggested bus model is re-analyzed according to the design criteria to ensure satisfaction of requirements. Longitudinal and lateral loads cause minimal stresses to the bus structure with inconsequential concentration near the passenger door. The first mode of the bus monocoque's natural frequencies is found to be 11.9 Hz. The frequencies for bending and torsion mode are increased from those of the baseline model to 16.6 Hz and 21.2 Hz due to higher stiffness of the structure. Comparisons of the structural performances calculated from the formulated equations and from FE analysis summarized in Table. 5 confirm accurate predictions of the responses. Rollover crash simulation indicates some damage areas due to transverse tension adjacent to the rear windshield window. However, the bus structure does not intrude into the survival space as can be seen from Fig. 15. In other words, the passenger safety is guaranteed under rollover accident.

<table>
<tr><td>Bottom part</td><td>Side panel</td><td>Floor</td><td>Pillar</td><td>Battery tray</td><td>Ceiling</td><td>Roof cover</td></tr>
<tr><td rowspan="2">G400,
t = 6 mm</td><td rowspan="2">G400,
t = 4 mm</td><td rowspan="2">G400,
t = 6 mm</td><td rowspan="2">G600, t = 6 mm</td><td>C200, t = 4 mm</td><td rowspan="2">G400, t = 6 mm</td><td rowspan="2">G400, t = 4 mm</td></tr>
<tr><td>G400, t = 2 mm</td></tr>
<tr><td>Foam,
t = 20 mm</td><td>Foam,
t = 20 mm</td><td>Foam,
t = 40 mm</td><td>Foam,
t = 30 mm</td><td>Foam,
t = 40 mm</td><td>Foam,
t = 50 mm</td><td></td></tr>
<tr><td rowspan="2">G400,
t = 6 mm</td><td rowspan="2">G400,
t = 4 mm</td><td rowspan="2">G400,
t = 6 mm</td><td rowspan="2">G600, t = 6 mm</td><td>G400, t = 2 mm</td><td rowspan="2">G400, t = 6 mm</td><td rowspan="2"></td></tr>
<tr><td>C200, t = 4 mm</td></tr>
</table>

Figure13: Materials assignment for the proposed model

Table5: Comparisons of structural responses obtained from established formulation and FE analysis

Responses	Eq. (7)	FEA	% Difference
M (kg)	1,783.3	1,782	0.1
K_B (N/mm)	36,772	36,487	0.8
K_T (N.m/deg)	111,998	102,329	9.4

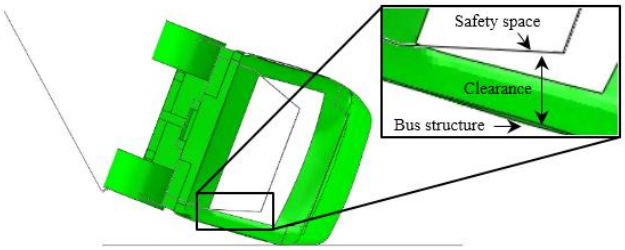

Figure14: Maximum deformation of bus structure and clearance between structure and survival area

4 Conclusion

This paper presents a parametric study and methodology to preliminarily design an 8-m electric bus structure for Thailand by using sandwich-structured composite. The sandwich structures comprising of foam core and E-glass and carbon faces are designed under design criteria on real driving conditions, stiffness requirements and crashworthiness performance under rollover. The bus structure is partitioned into seven design components based on investigations of stress distribution, load path and deformation characteristics under the prescribed load cases. Parametric study through thickness variations of core and face of sandwich structure delivers the level of significance in changing each design parameters to the specific stiffnesses of the bus monocoque. The equations for prompt prediction of structural performances are formulated to tailor the responses of interest. They are implemented together with parametric determination to improve the design of bus structure with respect to the stiffness requirements. The improved design meets with the required stiffnesses and its structural mass is practically reduced compared with existing buses. In the current work, the prediction of deformation in case of rollover accident in not considered and should be further investigated. Additionally, optimization process could be implemented to further minimize the weight of the structure and improve the design.

Acknowledgments

The authors gratefully acknowledge the financial support provided by the Thailand Research Fund (TRF), contract no. RDG6050041.

References

[1] The International Energy Agency, Global EV Outlook 2013, URL: http://www.iea.org/ publications/ globalevoutlook_2013.pdf, accessed on 29/10/2018.

[2] D. Croccolo, MD. Agostinis, and N. Vincenzi, “Structural Analysis of an Articulated Urban Bus Chassis via Finite Element Method: a Methodology Applied to a Case Study”, Journal of Mechanical Engineering, 57(2011)11, pp. 799-809.

[3] P. Kunakron-ong, K. Ruangjirakit and P. Jongpradist, “Design and analysis of electric bus structure in compliance with ECE safety regulations,” 2017 2nd IEEE International Conference on Intelligent Transportation Engineering (ICITE), Singapore, 2017, pp. 25-29.

[4] R. Jain, P. Tandon, and K. Vasantha, “Optimization methodology for beam gauges of the bus body for weight reduction,” Applied and Computation Mechanics, 8(2014), pp.47-62.

[5] J. B. Emmons, and L. J. Blessing, “Ultralight stainless steel urban bus concept,” SAE Technical Paper 2001-01-2073, 2001.

[6] P. Uttamung et.Al, “Light weight optimisation of electric bus body structure using finite element method,” Proceedings of the 7th TSME International Conference on Mechanical Engineering, Chiang Mai, Thailand, 2016, December 13-16.

[7] HY. Ko et. Al., “A study on the crashworthiness and rollover characteristics of low-floor bus made of sandwich composites”, Journal of Mechanical Science and technology, 23(2009), pp. 2686-2693.

[8] M. N. Velea, P. Wennhage, and D. Zenkert, “Multi-objective optimisation of vehicle bodies made of FRP sandwich structures,” Composite structures, 111(2014), pp.75-84.

[9] O. Testoni, “Concept and preliminary design for a composite monocoque for an electric city-bus”, Master thesis, Department of mechanical and process engineering, ETH Zurich, 2015, pp.1-88.

[10] United Nations Economic Commission for Europe, “Large Passenger Vehicles with Regard to the Strength of their Superstructure.”, United nations, 2007.

[11] BYD electric bus, http://www.byd.com, accessed on 2018-4-2

[12] Tindo E-Bus, http://www.cityofadelaide.com.au/assets/documents/FACTSHEET-tindosolar-bus.pdf, accessed on 2018-4-2

[13] King Long NJL6100, http://auto-che.com/v/njl/njl6100bev-247-dongyu.html, accessed on 2018-4-2

[14] TATA Ultra E-Bus, https://buses.cardekho.com/buses/tata/ultra-electric, accessed on 2018-4-2

[15] ALÉ E80, https://www.siemens.com/press/pool/de/events/2013/infrastructure-cities/2013-03-UITP-PK/background-ebus-wiener-linien-e.pdf, accessed on 2018-4-2

[16] Wuzhoulong Motors, http://www.wzlmotors.com/en/products-look.aspx?id=94, accessed on 2018-4-2

[17] Divinycell H, 2016, The high performance sandwich core, Diab Group.

[18] D. E. Malen., 2011. Fundamentals of Automobile Body Structure Design, SAE International, Pennsylvania, pp. 121-182.

[19] D. Shinabuth, “Finite Element Analysis of an Electric Bus Body Structure in Real Driving Conditions”, Proceedings of the 3rd TSME International Conference on Mechanical Engineering, Chiang Rai, Thailand, 2012, October 24-27.

[20] Z. Hashin. “Failure Criteria for Unidirectional Fiber Composites,” ASME J. Appl. Mech., 47(1980), 329-334.

Authors

Kitchanon Ruangjirakit received his M.Eng and Ph.D. in Aeronautical Engineering from Imperial College London, UK in 2008 and 2014, respectively. Currently, he is a lecturer at the Department of Mechanical Engineering, King Mongkut's Univeristy of Technology Thonburi, Bangkok, Thailand. His main research focuses on composite materials, design of lightweight automotive structure and energy consumption in electric vehicles.

Pathawee Kunakorn-ong is currently a researcher in the corporative project between King Monkut's University of Technology Thonburi (KMUTT), Thailand, and University of Ulsan, Korea, 'Design of Lightweight Structure for Electric Micro Bus in Thailand using Composite Materials'. He received his master's degree in mechanical engineering in 2017 from KMUTT and his research interests include: application of finite element method, optimization technique and structural analysis.

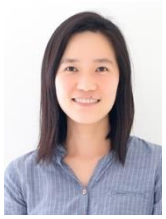

Pattaramon Jongpradist received her B.S. degree in Civil Engineering from Chulalongkorn University, Thailand, in 2001, M.Eng degree in Structural Engineering from Asian Institute of Technology, Thailand in 2003 and the Ph.D. degree in Mechanical Engineering from Memorial University, NL, Canada in 2007. From 2010 to 2014, she is an Assistant Professor and has been an Associate Professor since 2014 with the Department of Mechanical Engineering, King Mongkut's University of Technology Thonburi. Her research interests include computational mechanics, crash analysis and automotive design for safety.

Sontipee Aimmanee received his Bachelor of Engineering in Mechanical Engineering (First Class Honors, Gold Medal for 1st Rank GPA in college of engineering) in 1996 from King Mongkut's University of Technology Thonburi (KMUTT), Thailand, and Master of Science in Mechanical Engineering in 2000 from University of Delaware, USA, and Ph.D. in Engineering Mechanics in 2004 from Virginia Polytechnic Institute and State University, USA. Currently, he is an Assistant Professor at Department of Mechanical Engineering, Faculty of Engineering, KMUTT, Thailand. His research interests include mechanics of composite materials, sandwich structures, lightweight design, bio-inspired materials, structronics, and finite-element methods.

Yossapong Laoonual studied his first degree in Mechanical Engineering at Sirindhorn International Institute of Technology (SIIT), Thammasat University, Thailand. Between 1999 and 2006 he received Thai Government Scholarship to study in the UK where he continued his master's degree in Mechanical Engineering at the University of Manchester Institute of Science and Technology (UMIST), now University of Manchester, UK, followed by Imperial College London to gain his Ph.D. in Mechanical Engineering. He is currently an assistant professor at the Department of Mechanical Engineering, Faculty of Engineering, King Mongkut's University of Technology Thonburi (KMUTT). He is also one of founding members of Electric Vehicle Association of Thailand [EVAT) and currently the first elected President from 2015.